Quaternary Science Reviews 70 (2013) 1–14

Contents lists available at SciVerse ScienceDirect

Quaternary Science Reviews

journal homepage: www.elsevier.com/locate/quascirev

Invited review

Proglacial lake sediment records of Holocene climate change in the western Cordillera of Peru

Nathan D. Stansell [a,*], Donald T. Rodbell [b], Mark B. Abbott [c], Bryan G. Mark [a,d]

[a] Byrd Polar Research Center, The Ohio State University, Scott Hall Room 108, 1090 Carmack Road, Columbus, OH 43210, USA
[b] Geology Department, Union College, Schenectady, NY 12308, USA
[c] Department of Geology and Planetary Science, University of Pittsburgh, 4107 O'Hara St., Pittsburgh, PA 15260, USA
[d] Department of Geography, The Ohio State University, 1036 Derby Hall, Columbus, OH 43210, USA

A R T I C L E I N F O

Article history:
Received 21 November 2012
Received in revised form
1 March 2013
Accepted 5 March 2013
Available online

Keywords:
Southern tropical Andes
Glacier mass-balance
Glacial flour
Late Quaternary

A B S T R A C T

Sediment records from proglacial lakes between 9 and 10°S in the western Cordillera of the Peruvian Andes document the waxing and waning of alpine glaciers since the end of the Lateglacial stage. These records from the southern tropical Andes provide supporting evidence that the early Holocene (between 12 and 8 ka) was relatively warm and dry, and the middle Holocene (between 8 and 4 ka) was marked by a shift to cooler, and possibly wetter conditions in certain regions, leading to glacial advances. Although there were multiple periods of brief ice advances that interrupted the overall trend, glaciers in multiple valleys generally retreated from ~4.0 ka through the Medieval Climate Anomaly (1.0–0.7 ka). This late Holocene pattern of ice retreat occurred during a period when lake level studies, and both lacustrine and speleothem stable isotopic records indicate wetter conditions relative to the middle Holocene, suggesting that higher temperatures contributed to the pattern of ice retreat. Following this period of glacial retreat, multiple proxy records suggest that the start of the Little Ice Age (~0.6–0.1 ka) was a colder and wetter time throughout much of the tropical Andes. There appear to be two primary synoptic-scale climatic controls on temperature and precipitation linked to insolation dynamics that drive changes in ice cover in the southern tropical Andes during the Holocene: 1) the strength of the South America Summer Monsoon, which is linked to Northern Hemisphere temperatures and the mean position of the Intertropical Convergence Zone over the Atlantic, and 2) sea surface temperature distributions in the tropical Pacific Ocean and its influence on atmospheric temperature, precipitation and circulation patterns.

1. Introduction

Discerning the timing and causes of Holocene temperature and precipitation variations in the tropical Andes is important for our general understanding of global climate change (IPCC, 2007). The tropical hydrologic cycle, for example, plays a critical role in low-latitude climate dynamics through ocean and atmospheric circulation (Baker et al., 2001; Münnich and Neelin, 2005; Cruz et al., 2009), and our ability to predict future environmental changes linked to these processes requires a better understanding of how these parameters changed during the Holocene (Seltzer et al., 2000). Recent studies of glacier fluctuations document the timing and pattern of high-altitude environmental changes that are linked to ocean-atmospheric dynamics (Francou et al., 1995; Vuille et al., 2008a; Bradley et al., 2009; Rabatel et al., 2013). However, fundamental questions remain regarding the relative contributions of precipitation and temperature to glacier mass-balance in the tropical Andes, and the synoptic-scale mechanisms that caused the observed changes over longer, pre-instrumental time-scales (Jomelli et al., 2009).

Rodbell et al. (2008) provide a review of clastic sediment records from the tropical Andes, highlighting the potential for using proglacial lake sediment cores to document the history of glaciation, and discuss the potential mechanism for the observed changes. They focused on the timing and magnitude of variations in clastic sediment flux to proglacial lakes during the last local glacial maximum and Lateglacial stage (~30–10 ka). Many of the lake sediment records they used are from drainage basins that have been devoid of glaciers for the entire Holocene. Here, we build on this work by focusing on lakes from catchments in the western Cordillera of central Peru that are presently glacierized, and likely have been for much of the Holocene. A compilation of three lake

* Corresponding author. Tel.: +1 614 292 4910; fax: +1 614 292 4697.
E-mail addresses: stansell.9@osu.edu, nstansell@gmail.com (N.D. Stansell).

0277-3791/$ – see front matter © 2013 Elsevier Ltd. All rights reserved.
http://dx.doi.org/10.1016/j.quascirev.2013.03.003

sediment records, with west-facing slopes in the Cordilleras Blanca, Huayhuash and Raura, document changes in clastic sediment flux in their respective valleys since the end of the Lateglacial stage (ca 12 ka). We compare our findings with proxy reconstructions of regional precipitation (Baker et al., 2001; Cruz et al., 2009; Bird et al., 2011a; Strikis et al., 2011), ice core records (e.g. Thompson et al., 2006) and dated positions of paleo-ice margins (Buffen et al., 2009; Licciardi et al., 2009) in order to differentiate between the effects of temperature and precipitation on glacial variability during the Holocene.

2. Study site

2.1. Regional geology

The three proglacial lakes discussed in this study are from west-facing slopes of adjacent mountain ranges in the tropical Peruvian Andes that collectively form the NW-SE-trending, western-most glacierized cordillera of Peru (Fig. 1). From north to south, these ranges are the Cordillera Blanca, the Cordillera Huayhuash and the Cordillera Raura. The Cordillera Blanca is a ~200-km-long mountain range that is actively uplifting due, in part, to the prominent southwest-facing Cordillera Blanca Detachment Fault (McNulty and Farber, 2002). Modern glaciers in the Cordillera Blanca sit almost entirely on Miocene to Pliocene granite and granodiorite. There are also Cretaceous and Jurassic metasedimentary rocks that are mostly hornfels and quartzite (Clapperton, 1993). The Cordillera Huayhuash is located between the Cordillera Blanca and the Junin Plain. Most of the Huayhuash is southeast of the influence of the major normal faulting that is occurring in the Cordillera Blanca, and instead, thrust faulting and folding of Mesozoic sedimentary and metasedimentary rocks are evident along with Tertiary volcanic and intrusive rocks (Coney, 1971). Likewise, the Cordillera Raura exhibits thrust faulting and folding of rocks that are the similar in composition and age as those in the Huayhuash. The bedrock in these regions is mostly Cretaceous sedimentary and metasedimentary rocks, with some Tertiary volcanic and intrusive rocks, and descriptions of these units are found in Coney (1971), Cobbing et al. (1981), and Cobbing and Garayar (1998), with geochemical data in Stansell (2009).

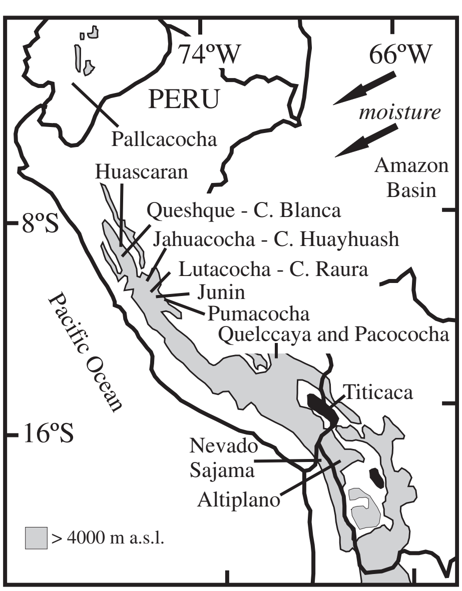

Fig. 1. Location map of sites discussed in the text. Shaded areas represent surface elevation greater than 4000 m asl. Arrows indicate predominant moisture-bearing easterly wind direction that causes higher precipitation on the eastern slopes of the central Peruvian Andes.

2.2. Laguna Queshquecocha – Cordillera Blanca

The Queshque massif is in the southern Cordillera Blanca, Peru (Fig. 2). The headwall of the watershed is ~5600 m asl. Laguna Queshquecocha (9°48′S, 77°18′W, 4260 m asl), with a maximum water depth of ~8.3 m, is dammed by moraines and outwash fans of the last local glacial maximum (Rodbell, 1991). Approximately 600 m up-valley from Laguna Queshquecocha is a smaller lake that is impounded by a Lateglacial moraine, dated by cosmogenic ^{10}Be to ~12.5 ka (Farber et al., 2005); a sediment record from this upper lake was discussed in detail in Rodbell et al. (2008). There are two glacierized drainages that feed sediment to the upper lake, with an outlet feeding lower Laguna Queshquecocha. The bedrock beneath the active glaciers is a combination of granodiorite and metasedimentary rocks, and glaciers advance to override proportionally higher amounts of granodiorite.

2.3. Jahuacocha – Cordillera Huayhuash

Laguna Jahuacocha (Fig. 3) is located on the west side of the Cordillera Huayhuash (10°14′S, 76°56′W, 4076 m asl). The headwall of the watershed is ~6406 m asl. The bedrock beneath the active glacier is dominated by carbonates and granitic intrusions, which contrasts markedly with the siliciclastic rocks that underlie the lake and much of the catchment that is not presently ice-covered (Coney, 1971). The lake is dammed by an end moraine that has been dated by cosmogenic ^{10}Be methods to the early Holocene (10.1 ± 0.9 ka; Hall et al., 2009). The Jahuacocha watershed has the greatest topographic relief and highest headwall elevation of the sites presented in this study. A prominent and very large moraine above Jahuacocha has not been dated, and it is possible that it is a compound moraine that was built during multiple glacial advances during the Holocene. The modern glaciers that provide meltwater and sediment to Laguna Jahuacocha are located mostly on the Santa Formation, which consists largely of carbonates, as well as granitic rocks. Bedrock beyond these active glaciers is dominated by the Carhuaz Formation that consists mostly of siliciclastic rocks.

2.4. Lutacocha – Cordillera Raura

Laguna Lutacocha (10°33′S, 76°43′W, 4320 m asl) is located in the southern Cordillera Raura (Fig. 4). The headwall of the watershed is ~5250 m asl. The lake is dammed by bedrock and has a water depth of ~6.5 m. The lake is the second in a series of three paternoster lakes that extend down-valley from an active glacier. The upper lake acts as a sediment trap, leading to the deposition of relatively fine-grained sediments in Laguna Lutacocha. There are multiple till deposits of varying ages in the Cordillera Raura, and most of these deposits have not been dated. Till in the vicinity of Laguna Lutacocha was initially interpreted as being Neoglacial by Clapperton (1972, 1983), although the deposits themselves have not been dated and could correspond to older events. These presumed Neoglacial till deposits extend down to an elevation as low as 4350 m, which is only ~30 m above the present shoreline of Laguna Lutacocha. This implies that meltwater from glaciers would have been flowing directly into the lake at times of glacial advances, resulting in changes in the composition of sediments being deposited. Topographic maps from A.D. 1965 identify multiple glaciers in the northeast and southwest quadrants of the watershed, but only one glacier in the northeast remains today (McFadden et al., 2011). The modern glacier for Lutacocha is located on the Jumasha limestone that consists of bioclastic and pelletal

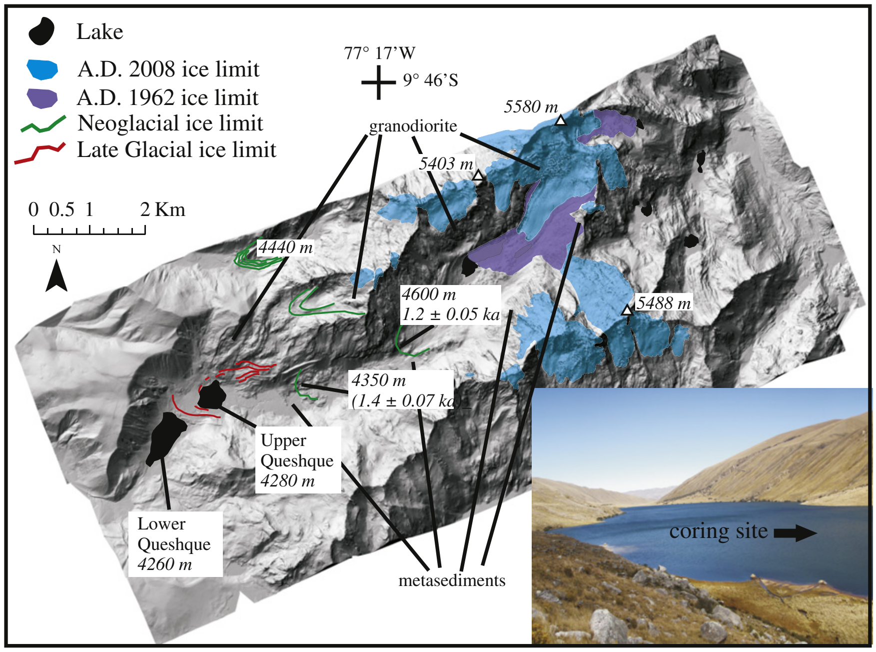

Fig. 2. Shaded relief map of the Laguna Queshquecocha watershed and photograph of coring site in the lower lake (inset) with present-day ice limits generated from LiDAR data collected in 2008. The mapped positions of the A.D. 1962 ice limits are from Mark and Seltzer (2005). A moraine that impounds the upper Laguna Queshquecocha has been dated to the Lateglacial stage (Farber et al., 2005). Pre-LIA Neoglacial moraines in the main Queshque valley are situated above the Queshquecocha lakes (Röthlisberger, 1987; Rodbell et al., 2008). The other mapped Neoglacial and Lateglacial stage ice limits are also indicated. The bedrock beneath the active glaciers is a combination of granodiorite and metasediment rocks, and glaciers advance to erode proportionally higher amounts of granodiorite.

limestone and dolomite with layers of fine-grained carbonate and rare calcareous siltstone. Bedrock beyond the active glacier includes interbedded gray and brownish shale, calcareous shale, bituminous shale, siltstone, sandstone, quartzite and limestone. Although not formally mapped in the Lutacocha watersheds, our fieldwork identified Tertiary intermediate composition flows and pyroclastic rocks that are similar to what has been identified in nearby valleys (Cobbing and Garayar, 1998).

2.5. Modern climate and conditions that affect glacier mass balance

The climate of the tropical Andes is typical of low latitudes, where the diurnal temperature range is greater than the annual range. Precipitation is derived mostly from Atlantic Ocean moisture that is transported to the Andes via the easterlies (Garreaud et al., 2009). Seasonal rainfall variability in the

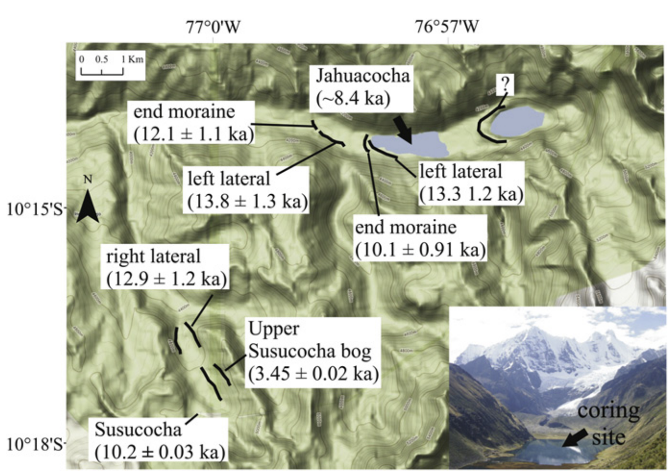

Fig. 3. Shaded relief image of the Laguna Jahuacocha watershed and adjacent regions in the Cordillera Huayhuash. The coring site at Laguna Jahuacocha is indicated in the inset photograph. The bedrock beneath the active glacier is mostly carbonate rocks with granitic intrusions, whereas the rocks that underlie the non-glacierized portions of the catchment are dominantly siliciclastic. The ages of moraines and basal ages from lakes and bogs are reported in Hall et al. (2009), Rodbell et al. (2009) and this study. Although discontinuous, these ages suggest that ice retreated at the end of the Lateglacial stage and remained at elevations above Laguna Jahuacocha throughout the Holocene. There is a prominent moraine up-valley from Laguna Jahuacocha that has not been dated, and is possibly a compound feature of middle and late Holocene ice advances.

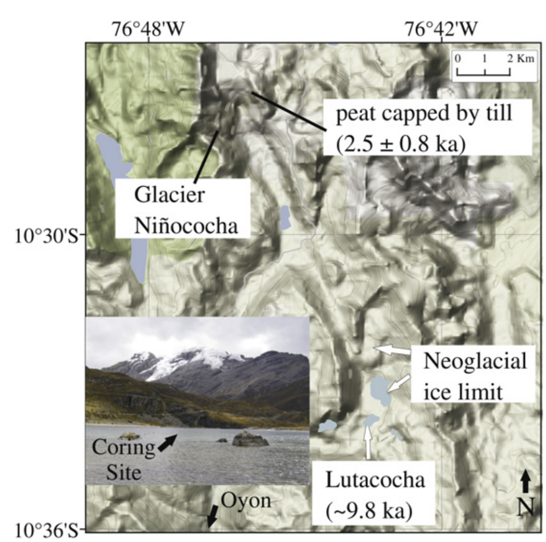

Fig. 4. Shaded relief image and photograph (inset) of the Laguna Lutacocha watershed and surrounding Cordillera Raura. The bedrock beneath the active glacier is mostly limestone (above ~4600 m asl), whereas that underlying the non-glacierized portions of the catchment is dominated by siliciclastic rocks and sedimentary units of mixed composition. Clapperton (1983) reported ages of 2.5 ± 0.8 ka for peat capped by till approximately 800 m in front of Glacier Niñococha. The Neoglacial ice limit was mapped by Clapperton (1972), although absolute ages have not been assigned.

tropical Andes is linked to the position of the Intertropical Convergence Zone (ITCZ) over the Pacific and Atlantic Oceans, and by the strength of the South American Summer Monsoon (SASM) over the Amazon Basin (Zhou and Lau, 1998; Maslin and Burns, 2000; Maslin et al., 2011; Vuille et al., 2012). Inter-annual and multi-decadal rainfall patterns and temperature fluctuations over South America are affected by variability in mean-state conditions in the Atlantic and Pacific Oceans (Johnson, 1976; Nobre and Srukla, 1996; Henderson et al., 1999; Vuille et al., 2000; Bradley et al., 2003; Vuille and Werner, 2005). For example, the warm phase of the El Niño Southern Oscillation (ENSO) typically produces higher wet season rainfall amounts at low elevations along the Pacific coast of Peru, and the opposite during cold phases (Coelho et al., 2002). At altitude, glaciers are affected by ENSO through large-scale circulation dynamics and zonal flow anomalies in the upper troposphere that affect snowfall (Vuille et al., 2008b). Detailed meteorological data for the Cordilleras Raura and Huayhuash are currently lacking, but monthly records since A.D. 1948 are available for the nearby Cordillera Blanca. Although the relationship breaks down during certain years, El Niño events generally cause warm and dry conditions, whereas La Niña events are cold and wet in alpine regions of the southern tropical Andes (Vuille et al., 2008b). In addition, precipitation amounts are affected by positive sea-level pressure anomalies in the North Atlantic Ocean, as these usually result in a displacement of the ITCZ and a shift in the strength of the SASM (Chiessi et al., 2009). Cloud cover data from satellite imagery, and relative humidity values from station data also indicate a seasonal pattern, with generally higher levels during the wet season (Fairman, 2006).

Aspect and the orientation of glaciers in the western Cordillera of South America are largely controlled by the structural trend of the Andes, and also reflect regional gradients in precipitation and solar radiation (Hastenrath, 2009). The NW–SE trend of the mountain ranges in central Peru generally explains the distribution of glaciers (Kaser and Georges, 1997). While precipitation moisture originates from easterly winds, the local geologic structure of the Cordillera Blanca and resulting diurnal shading favors the development of more and larger glaciers in SW facing valleys like Queshque (Kaser and Georges, 1997; Mark and Seltzer, 2005). On the western side of western Cordillera, where our work is focused, mean annual precipitation decreases with decreasing elevation, producing arid conditions below 2000 m asl altitude (Seltzer, 1992). For example, an average of ~1200 mm/yr of water-equivalent frozen precipitation falls on the existing glaciers in the Cordillera Raura (station elevation: 4900 m asl) (Ames and Hastenrath, 1996), and only ~520 mm/yr of precipitation occurs at a meteorological station in the town of Oyon, ~10 km southwest of the Lutacocha watershed (3600 m asl) (Lawrimore et al., 2011).

The mass balance of glaciers in the tropical Andes responds to both temperature and precipitation changes. From a glaciological perspective, the western Cordillera of central Peru (~8–11°S) is intermediate between the inner and outer tropics, with precipitation and humidity being seasonal, yet high enough to limit substantial ice loss to sublimation (Kaser and Osmaston, 2002). The dominant mode of ablation in these regions is melting, and the equilibrium line altitude (ELA) of glaciers mimics the local freezing level height (or 0 °C isotherm). Modern temperature values and radiosonde observations indicate that ELA's in the central Andes have risen by at least ~70 m since ~A.D. 1962, as a consequence of warming temperatures (Mark and Seltzer, 2005). At the same time, precipitation has decreased, accelerating the rate of recent glacial retreat (Vuille et al., 2008b).

3. Methods

3.1. Fieldwork

Proglacial lakes in the western Cordillera of Peru that contain continuous sediment records through the Holocene were targeted for coring and analyzes. Water depth at each site was measured by sonar prior to coring. A 1090-cm-long composite sediment core was taken from the depocenter (8.3 m) of Laguna Queshquecocha in 2009 using a square-rod piston corer (Wright et al., 1984), and stored in split PVC tubes in the field. A surface core was also collected from nearly the same location using a piston and polycarbonate tubing in order to capture the flocculent material that comprises the sediment–water interface. The top 25 cm of the surface core were sampled in the field at 0.5-cm intervals. Similarly, a 582-cm-long composite sediment core was collected from Laguna Lutacocha in 2006 (water depth: 6.5 m) also using a square-rod piston corer, and we were able to collect the modern section of the record in split PVC. Likewise, a ~1200-cm-long composite core that included the modern section of the record was collected from Jahuacocha in 2003 (water depth: 3.5 m) using a square-rod piston corer and stored in split PVC. Glacial till and bedrock samples were collected from exposed units in each watershed for geochemical analysis, and to characterize the source material for clastic sediments that accumulate in the studied lake basins.

3.2. Geochronology

The sediment chronology for each lake is based on radiocarbon ages of charcoal and aquatic macrofossil samples that were picked under a binocular microscope (Table 1). Samples were pre-treated using standard acid–base–acid protocols (Abbott and Stafford, 1996), and measured using accelerator mass spectrometry at the Keck Radiocarbon facility at the University of California, Irvine. Radiocarbon ages were then calibrated and converted to calendar ages (with present defined as A.D. 1950) using Oxcal version 4.1 and the Intcal 09 dataset (Reimer et al., 2009). Age–depth models are based on polynomial functions for median ages that were generated using Bayesian statistical methods and the depositional model program in Oxcal (Fig. 5) (Bronk Ramsey, 2008). The Queshquecocha core was also measured for ^{210}Pb activity (Oldfield and Appleby, 1984) at the University of Pittsburgh.

3.3. Sedimentology and geochemistry

Multiple methods were used to measure the geochemistry for each sediment core. First, the sediments were analyzed using an ITRAX scanning X-Ray Fluorescence (XRF) instrument (Croudace et al., 2006; Rothwell and Rack, 2006) at the Large Lakes Observatory at the University of Minnesota, Duluth. The sediments were measured by XRF at 1- to 4-mm spacing with 30-s exposure time for each interval. Between 30 and 50 freeze-dried samples from 1-cm-thick sections of the Queshquecocha and Lutacocha sediment cores were also analyzed by the ALS Chemex commercial facility in Reno, Nevada using both ICP-MS and ICP-AES in order to convert XRF values (counts per second) to units of concentration. This also enabled us to merge the geochemical data from the extruded Queshquecocha samples with the longer sediment record that was measured by scanning XRF. The Jahuacocha geochemical data were not converted to concentrations and are presented here as counts per second (CPS). Magnetic susceptibility (MS) was measured at a 2- to 5-mm interval using a Tamiscan high-resolution surface-scanning sensor connected to a Bartington susceptibility meter either at the University of Pittsburgh or at Union College. In addition, total inorganic carbon (TIC) and total carbon (TC) values were

Table 1
Radiocarbon ages used in this study. The calibrated age ranges were calculated using OxCal v4.2 and the Intcal 09 dataset (Bronk Ramsey, 2008; Reimer et al., 2009). The modeled ages are the result of the depositional model method within the OxCal program. The range represents the 2-sigma values, and the median ages are in parentheses.

Lab #	Depth (cm)	Measured ^{14}C age	Measured error (±)	2 σ calibrated age (cal yr BP)	Oxcal modeled age (cal yr BP)
Queshquecocha					
UCI-75960	68	390	25	326-(469)-509	327-(470)-509
UCI-75961	129	1340	30	1182-(1279)-1307	1181-(1277)-1307
UCI-75962	172	1705	30	1542-(1610)-1695	1545-(1615)-1697
UCI-75963	304	3110	20	3265-(3347)-3383	3263-(3344)-3382
UCI-75964	471	4200	30	4627-(4735)-4893	4645-(4749)-4846
UCI-75984	520	4650	35	5309-(5404)-5469	5310-(5399)-5467
UCI-75985	703	6670	55	7435-(7538)-7650	7460-(7550)-7658
UCI-75986	782	8520	50	9453-(9511)-9551	9452-(9510)-9551
UCI-75987	1064	13,130	45	15265-(15,946)-16486	15164-(15,682)-16321
Jahuacocha					
UCI-113089	183	1140	30	968-(1033)-1169	978-(1058)-1172
UCI-113090	331	3065	35	3169-(3290)-3369	3165-(3279)-3365
UCI-113091	377	3480	70	3575-(3755)-3958	3475-(3642)-3784
UCI-113092	705	4355	40	4845-(4924)-5039	4851-(4935)-5039
UCI-113093	797	4635	20	5310-(5418)-5450	5305-(5322)-5442
UCI-113094	900	4730	70	5319-(5467)-5590	5495-(5575)-5710
UCI-113095	930	5100	100	5607-(5836)-6174	5654-(5773)-5897
UCI-113096	966	5195	15	5915-(5942)-5990	5917-(5956)-5991
UCI-113097	1061	6245	30	7026-(7196)-7258	7028-(7197)-7258
UCI-113098	1119	7210	110	7828-(8040)-8311	7719-(7926)-8096
UCI-113099	1171	7410	140	7956-(8225)-8506	8030-(8209)-8369
UCI-113100	1201	7520	110	8052-(8323)-8546	8197-(8363)-8541
Lutacocha					
UCI-22772	61	520	25	510-(530)-622	475-(486)-503
UCI-37625	77	205	40	0-(180)-310	481-(492)-504
UCI-37626	89	520	25	510-(530)-622	509-(533)-621
UCI-37627	109	930	30	781-(850)-926	778-(847)-925
UCI-37628	137	1260	30	1088-(1210)-1281	1090-(1214)-1281
UCI-22773	182	2000	30	1880-(1950)-2035	1829-(1896)-1935
UCI-37541	202	1935	20	1825-(1880)-1929	1878-(1920)-1986
UCI-22850	227	2435	35	2353-(2480)-2701	2354-(2478)-2700
UCI-25181	254	3030	30	3084-(3250)-3345	3157-(3253)-3350
UCI-22851	292	4615	30	5292-(5410)-5461	5083-(5327)-5457
UCI-32730	576	8330	60	9136-(9350)-9476	9140-(9356)-9483
UCI-25180	131	370	20	427-(450)-500*	*Omitted

measured for all 3 cores by coulometry (Englemann et al., 1985; Dean, 1999) every 3–5 cm down core. Total carbon was measured by combusting samples at 1000 °C using a UIC 5200 automated furnace, and TIC was measured by acidifying samples in 1.0 N $HClO_4$ using a UIC 5240 acidification module; the carbon dioxide liberated in both cases was measured using a UIC Coulometrics™ carbon dioxide coulometer in the Core Analysis Laboratory at Union College. Finally, weight percentage total organic carbon (TOC) was calculated by subtracting TIC from TC (TOC = TC-TIC).

The till matrix ($n = 8$) and bedrock samples ($n = 12$) collected from the Queshquecocha watershed were analyzed using ICP-MS methods at Union College (Moy, 1998). The till matrix ($n = 3$) and bedrock ($n = 9$) samples representing the exposed units in the Lutacocha and Jahuacocha watersheds were collected in 2006, and the samples were sent to the ALS Chemex commercial facility in Reno, Nevada where they were crushed, pulverized, digested using four-acid (near total) methods and measured for elemental chemistry using both ICP-AES and ICP-MS (Stansell, 2009).

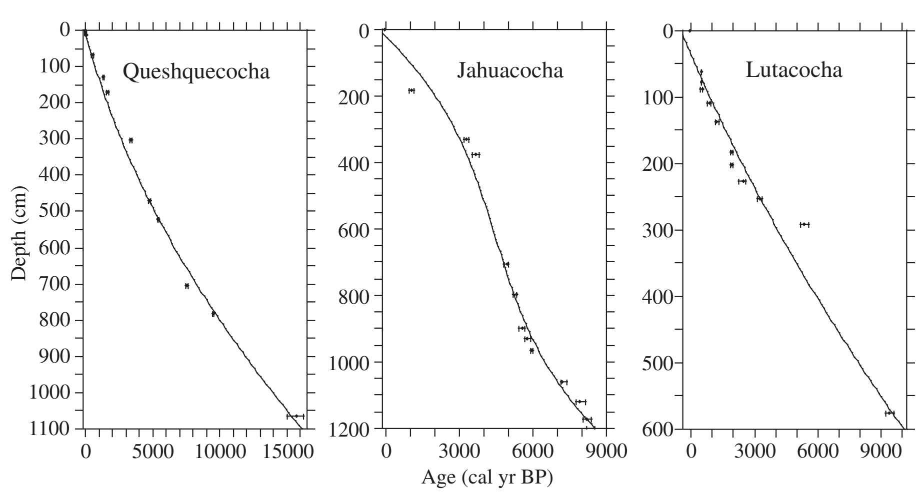

Fig. 5. Age–depth models using polynomial functions for sediment cores discussed in text. The ages represent the median values from the depositional model program in OxCal and the error bars represent the 2-sigma values (Table 1).

Discrimination plots of Ti, Fe and Ca, and bivariate plots of Fe and Ca were made to highlight the contrasting chemical compositions of the samples collected (Fig. 6).

3.4. Biogenic silica

Weight percentage biogenic silica ($bSiO_2$) was measured on freeze-dried samples at the Union College Core Analysis Laboratory. Samples were collected from centimeter-thick sections, taken every 10–20 cm down-core. A modified wet alkali sequential digestion method (DeMaster, 1979, 1981; Conley, 1998) was used on approximately 10 mg of freeze-dried sediment (Conley and Schelske, 2001), which allows for separation of $bSiO_2$ from the minerogenic and aluminosilicate fraction. Aliquots of the supernatant of each sample in a hot 0.1 M NaOH solution were extracted after reaction times of 2, 3, 4, and 5 h, and each of these were analyzed for Si by ICPMS. The time-dependent release of SiO_2 was modeled by a linear best fit line, and the *Y* intercept of the resultant equation was taken to indicate the biogenic component, following Conley and Schelske (2001).

3.5. Percent clastic sediment and stacked record of clastic sediment flux

We followed the approach of Rodbell et al. (2008) in order to compile the multiple clastic sediment records from lakes with headwall elevations >5000 m in the Peruvian Andes (Fig. 10). This compilation includes the 3 records presented here as well as Lake Huarmicocha from the Cordillera Huayhuash that was also included in the compilation by Rodbell et al. (2008). The clastic sediment component for all records was calculated as the fraction remaining after subtracting organic matter (converted to organic matter by multiplying % organic carbon values by 1.72) and biogenic silica from the total dry sediment bulk density. Biogenic silica concentrations for the Huarmicocha record of Rodbell et al. (2008) are <1% and are considered negligible. Clastic sediment for all records was converted to flux ($g/cm^2/yr$) by multiplying the clastic component of dry bulk density (g/cm^3) by sedimentation rate (cm/yr). These time-series were then re-sampled at even 100-year time increments using the spline interpolation function in MATLAB (Trauth, 2010). Next, each re-sampled clastic sediment flux value was converted to units of standard deviation (*z*-scores) from the mean values for each sediment core. These re-sampled *z*-score values were then averaged to produce a stacked record of clastic sediment flux.

4. Results

4.1. Sedimentology

The sediments from all three lakes are angular to sub-rounded silts to fine sands, indicating that most of the material is minerogenic and detrital. In all three records, organic matter is low (generally <4%), and biogenic silica concentrations (<10%) covary with organic matter. The majority of the sediments in the cores from Laguna Queshquecocha are laminated at millimeter-scale (Fig. 7), alternating between mostly light to dark gray (Gley 5/1) with intermittent layers that are yellowish gray (5Y 8/2). Sediments from Laguna Jahuacocha are mostly massive, light gray (10YR 7/1) with intermittent layers that are light yellowish brown (2.5Y 6/4) (Fig. 8). Sections of the Lutacocha sediment core that date to between ~9.8 and 4.0 ka contain mostly massive, dark gray sediment that is capped by a ~10-cm-thick yellowish-brown and grayish brown sequence of mostly sand-sized material. This sharp contrast is represented in the sediment record as an abrupt geochemical transition at ~4.0 ka (Fig. 9). The majority of the Lutacocha sediment core younger than ~4.0 ka is laminated at millimeter-scale, alternating between mostly gray (Gley 5/1) and yellow (5Y, 8/2) layers, with intermittent greenish-gray (Gley 4/2), olive brown (2.5Y, 4/3) and grayish brown (2.5Y, 3/1) sections. Hereafter, we refer to sediment that is mostly gray and silt-clay rich as glacial flour.

4.2. Geochemistry and clastic sediment flux

The Queshquecocha core provides a continuous sediment record that spans the entire Holocene, and Fig. 7 illustrates multiple

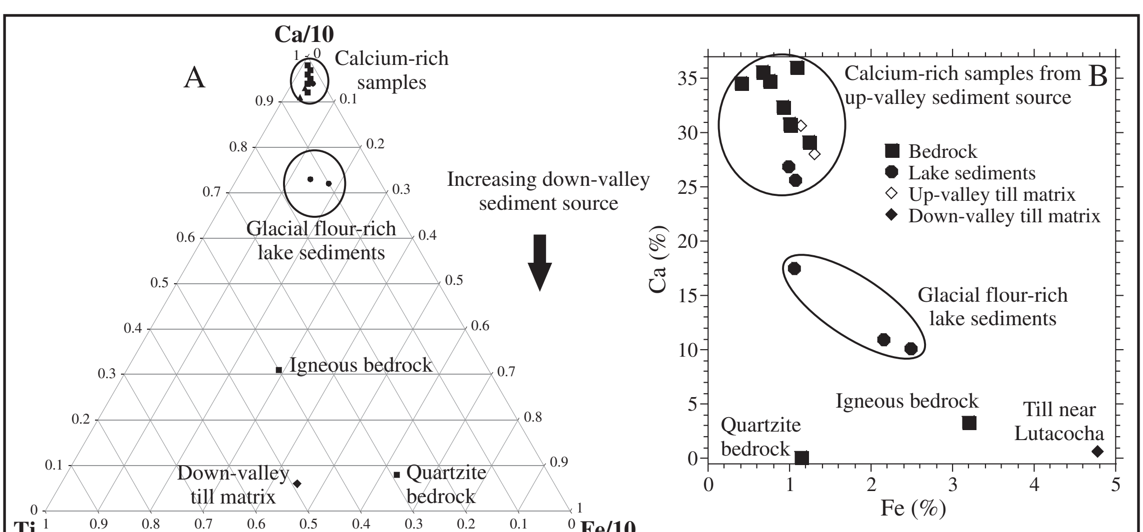

Fig. 6. Discrimination plots of bedrock and bulk sediment geochemical data from the Cordillera Raura. Inset A is a ternary diagram illustrating the relationship between Ca, Fe and Ti concentrations of the bedrock, till and lake sediment samples collected from the Lutacocha watershed. Inset B is a bivariate plot of Fe and Ca. The Ca-rich samples were collected from regions at high elevations in the watershed. The samples with relatively high Fe and Ti concentrations represent the down-valley locations. The sections of the lake sediment core with high glacial flour concentrations and the till matrix samples have proportionally high amounts of Fe and Ti, and indicate that a shift in provenance occurred during periods of ice advance. A till matrix sample collected near the margin of Lake Lutacocha has the highest Fe and lowest Ca concentrations of all the measured samples, and represents the glacial sediment end-member.

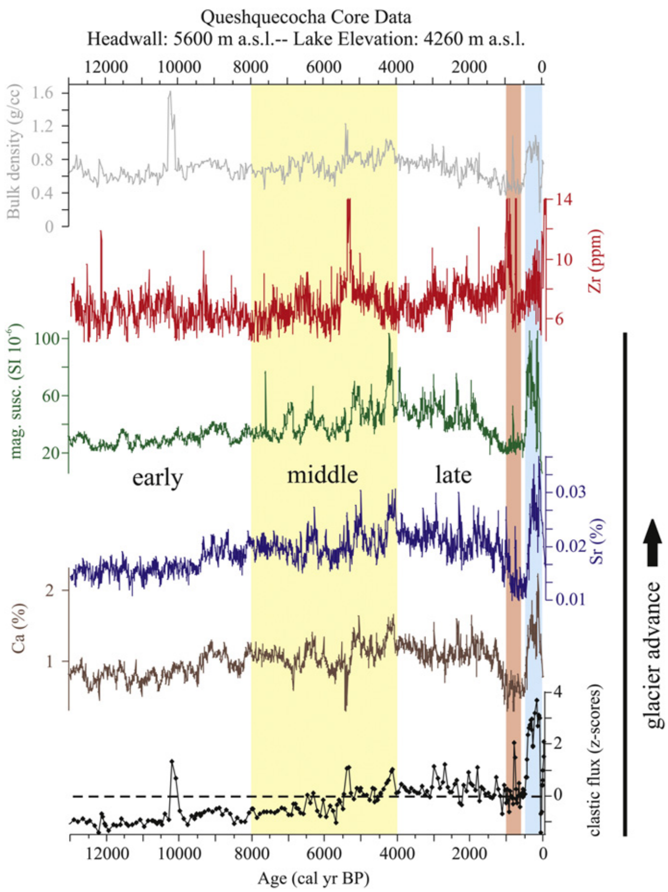

Fig. 7. Sediment core data plotted versus age from Laguna Queshquecocha in the Cordillera Blanca with shading in yellow for the middle Holocene, red for the MCA and blue for the LIA. Periods of overall ice advance are represented by higher values of bulk density, magnetic susceptibility, Sr, Ca and clastic sediment flux whereas periods of retreat are generally characterized by decreasing values of these proxies and higher amounts of Zr. Glaciers progressively advanced above Laguna Queshquecocha from ~10.0 to 2.0 ka followed by retreating ice margins until 0.5 ka. Glaciers were relatively advanced again from 0.5 ka until modern.

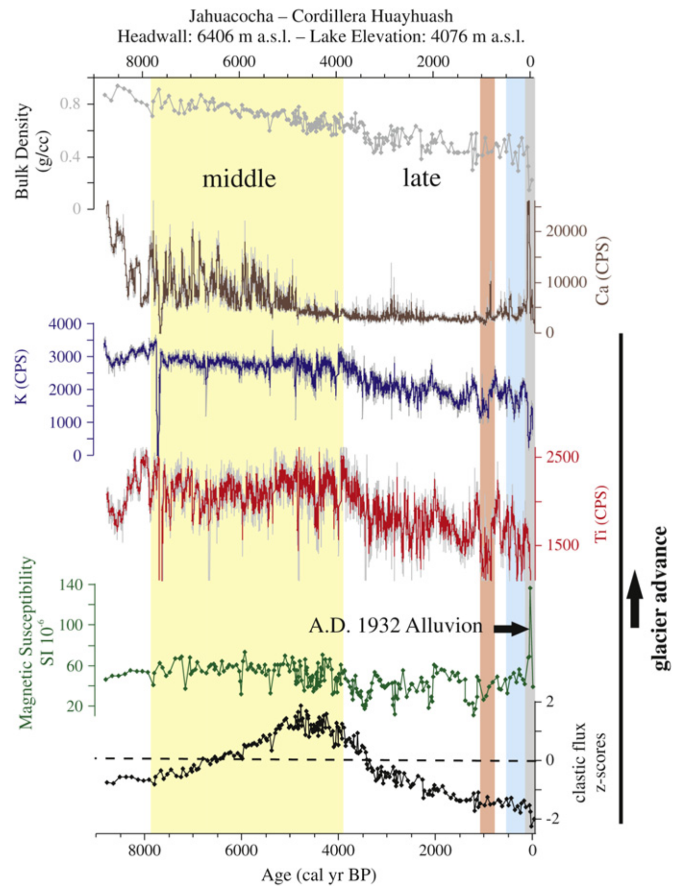

Fig. 8. Sediment core data plotted versus age from Laguna Jahuacocha in the Cordillera Huayhuash with shading in yellow for the middle Holocene, red for the MCA and blue for the LIA. Glaciers were advancing during periods of increasing Fe, Ti, magnetic susceptibility and clastic flux values and decreasing Ca values. The gray lines in the Ca, Fe and Ti plots represent the raw values and the color is the 10-point moving average. The sediment core records phases of ice retreat during periods when Ti, Fe, Ca, magnetic susceptibility and clastic sediment flux covary and decrease. Glaciers were advancing during the early and middle Holocene followed by ice retreat through most of the remaining late Holocene. There was a brief re-advance centered around 0.5 ka.

geochemical variables that serve as proxies for changing sediment sources through time. Profiles of bulk density, Ca, Sr, MS and clastic sediment flux all covary through most of the record. Clastic sediment flux values are low and exhibit little variability starting at ~13 ka and during the early Holocene, followed by a trend to higher values from ~7.0 to 4.2 ka. Clastic sediment concentrations remain high in the late Holocene, but there is a slight trend toward lower values from 2.0 ka through the Medieval Climate Anomaly (MCA; red shading on Fig. 7) followed by a shift to higher values in the last ~500 years of the record that contains the Little Ice Age (LIA, blue shading on Fig. 7).

The Jahuacocha core captures a continuous record of sedimentological changes in the watershed during the last ~9000 years (Fig. 8). Bulk density values exhibit an overall decreasing trend from 9.0 ka until the present (Stevens, 2004). However, clastic sediment flux values increase from ~9.0 to 5.0 ka, followed by decreasing values through most of the remaining Holocene. Values for MS, Ti and K are consistently high or increase during the early and middle Holocene until ~4 ka. After ~4.0 ka, there is a decreasing trend in these proxies through the remaining Holocene with the exception of multiple, centennial-scale periods of increasing values. In general, Ca values are higher in sections of the core with lower Ti and K values, and Ca values generally decrease from ~9.0 to 4.0 ka followed by low but variable values through most of the remaining Holocene. The most recent 300 years of the record reveals a trend of slightly higher values of Ti, K, MS and clastic flux, although a sharp increase in clastic sediment concentration values in the upper ~5 cm of the core reflects an alluvion that was historically documented in A.D. 1932.

The Lutacocha record contains a continuous sediment sequence spanning the last ~9800 years (Fig. 9). Peaks in clastic sediment flux correspond with peaks in MS, Ti and Fe, and with intervals that are low in Ca. The geochemical data identify two major down-core end member compositions within the lake sediments. First are sediments that are dominated by detrital calcium carbonate, with low Ti, Fe, bulk density and clastic sediment flux. Second are sections of the core with low Ca and high clastic sediment flux values that likewise have high Fe and Ti values. Sections of the core with high Ti, Fe and clastic flux values generally decrease in frequency from ~9.8 to 6.0 ka followed by increasing frequencies that peak at ~4.7 ka. Clastic sediment flux values sharply decreased after ~4.0 ka followed by variable and generally low values until 0.4 ka. Notably, in the upper section of the record there is a ~10-cm-thick band of fine-grained gray clay sediment with high Ti, Fe, and clastic sediment flux that centers on ~0.3 ka.

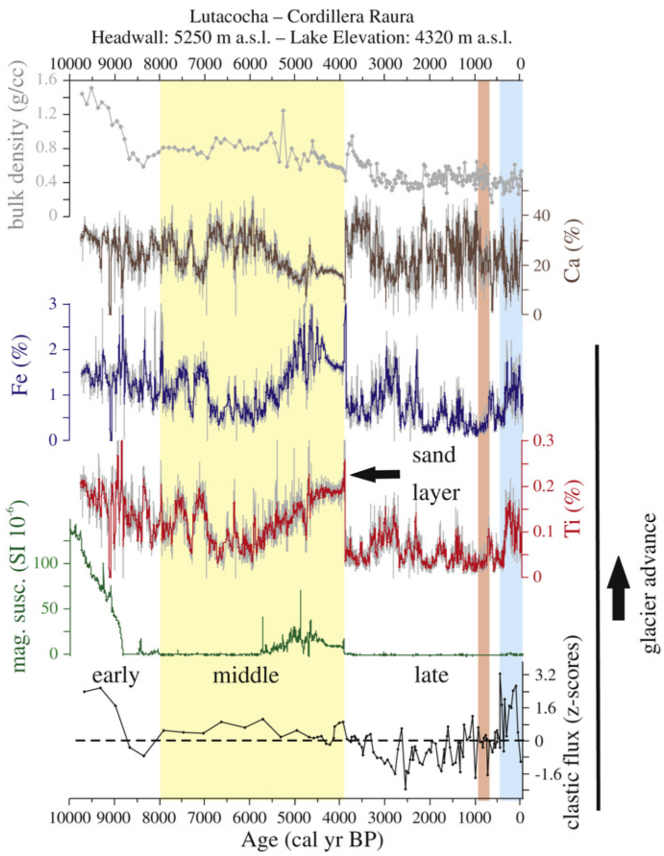

Fig. 9. Sediment core data plotted versus age from Laguna Lutacocha in the Cordillera Raura with shading in yellow for the middle Holocene, red for the MCA and blue for the LIA. The gray in the Ca, Fe and Ti plots represents the raw values and the color is the 10-point moving average. Higher Fe, Ti, magnetic susceptibility and clastic sediment flux values, and decreasing Ca values, represent periods of glacial advance and vice versa. Ice margins retreated from ~10.0 to 8.5 ka followed by overall advanced ice margins until ~4.0 ka. The abrupt transition at ~4.0 ka marks the boundary between massive gray sediments capped by a sand layer below and laminated sediment above. The late Holocene is marked by fluctuating, but overall retreating ice margins punctuated by a pronounced re-advance centered on 0.3 ka.

5. Discussion

5.1. Interpreting sedimentological changes in proglacial lakes

Previous lake sediment studies in the tropical Andes have identified systematic variations in sediment yield that reflect changes in the extent of climate-mediated up-valley ice cover (Abbott et al., 2003; Stansell et al., 2005; Polissar et al., 2006b; Rodbell et al., 2008; Stansell et al., 2010). In the tropical Andes, glaciers have short response times to changes in net balance, as demonstrated by the synchrony of hydrologically-derived mass balance with observations of terminus positions (Kaser et al., 2003). Therefore, during periods of glacial advance sediment yield is greater than in periods of glacial retreat. Likewise, variation in down-core proxies for clastic sediment, including physical properties, geochemistry and magnetic susceptibility show changes characteristic of increased or decreased glacial activity depending on whether the glacier is advancing or retreating, and can be used to date the timing of past changes in glacier mass-balance.

Following the above process model, we combine dated sediment cores with geochemical data to calculate clastic sediment flux and interpret times of high clastic yield to indicate periods of glacial advance. The increased clastic sediment flux reflects active erosion by the growing glacier, whereas a decrease clastic sediment flux reflects ice margin retreat and lower erosion rates (Harbor and Warburton, 1992). There is likely a short time lag between changes in the glacier and shifts in the flux of clastic sediment, especially as moraines degrade following a period of ice retreat (Jansson et al., 2005; Benn et al., 2006); however this offset in timing is likely negligible (<10 years) in the small, Andean catchments, as glacier termini are proximal to lake basins. Moreover, glacier retreat can generate high rates of paraglacial sediment yield when erosion of glacially derived sediment occurs on the steep, unvegetated landscapes (Smith and Ashley, 1985; Benn et al., 2006; Nussbaumer et al., 2011). However, this is limited for the sites in our study because small warm-based glaciers have large amounts of water constantly draining, thus limiting the amount of fine-grained sediment accumulating at their base. Past work has shown that higher rates of clastic sedimentation in proglacial lakes are correlated to multi-decadal to century-scale periods of ice advance rather than retreat (e.g. Leonard, 1997). On the time scale of centuries, Rodbell et al. (2008) concluded that the major first order control on sediment yield from tropical Andean catchments is the extent of glacial ice in the catchment.

In addition to glacial processes, clastic sediment flux to Andean lakes can also shift in response to changes in precipitation amount with or without any glacigenic sediment input. It should be noted, however, that with the exception of Lake Pallcacocha, Ecuador (Fig. 1), most Andean catchments that were not glaciated during the Holocene show little or no pronounced changes in clastic sediment flux over the last ~10 ka (Rodbell et al., 2008). If precipitation changes were the primary factor that controlled clastic sedimentation in these systems over the Holocene, then records from both glaciated and non-glaciated valleys would reveal a similar pattern. Lake sediment records from catchments with headwall elevations <5000 m show markedly lower rates of clastic sediment input than do records from lakes with headwalls >5000 m (Rodbell et al., 2008). This latter provides further evidence that glacial processes, and not precipitation, are likely responsible for the major changes in sediment composition presented in this study.

We examined multiple variables in lake sediment cores as proxies for changes in sediment source, to interpret past changes in glacial variability in addition to clastic sediment flux values. The geology and main geochemical proxies for glacial flour vary among watersheds, and while we rely mostly on the clastic sediment flux data for our interpretations, the other proxies provide supporting evidence of past glacial variability. For example, in the Queshquecocha watershed we used geochemical measurements to determine that bedrock varies at different elevations in the catchment as well as till-matrix and moraine samples. These end-members have significantly different concentrations of Sr, Ca and Zr (Moy, 1998), and these findings combined with results from scanning XRF measurements on lake sediment cores help identify the source of the sediment and how this may have changed as glaciers advanced and retreated. We found that the bedrock near the glacier headwall is comprised mostly of metasediments with high concentrations of Zr, whereas the granodiorite in the valley below and in adjacent regions has higher concentrations of Sr and Ca. In the Queshquecocha watershed, variations in the end-members of Sr and Ca versus Zr in the lake sediment cores represents shifts in the source of the sediment and this change can be attributed to shifts in the material being eroded by glaciers as they advance and retreat. As noted above, we assume that glacial systems are the dominant source of erosion in the Cordillera Blanca, and changes over time in the chemical composition of the sediment in the Queshquecocha cores reflect changes in up-valley glacier surface area. When glaciers advance leading to increased erosion of the lower elevation bedrock Zr values are diluted by higher concentrations of Sr and Ca. Thus, higher Sr and Ca values in the core represent periods of glacial advances, whereas higher concentrations of Zr indicate times of smaller, more restricted glaciers. Higher Sr and Ca values also correspond to periods of higher magnetic susceptibility, bulk density and clastic sediment flux, which are also indicators of greater glacial erosion during periods of advancing glaciers.

The active glaciers above Jahuacocha and Lutacocha sit mostly on carbonate rocks, and a mix of bedrock units are situated down-valley (see Section 2.1). For Lutacocha, Ca and Ti are used as proxies for changes in the proportion of glacial and non-glacial sediments because there are sharply contrasting concentrations of these elements in bedrock samples from different elevations underlying the glaciated area of the catchment, and they are also the major elements found in the sediment cores. The Lutacocha sediment that is high in Ti is also high in Fe, which is characteristic of the volcanic rocks down-valley of the active glaciers in that watershed. The Jahuacocha sediment that is high in Ti is also high in K, which is characteristic of the siliciclastic rocks below the active glaciers in the watershed. Periods of ice advance in both records are marked by a shifting proportion to higher Ti (and Fe or K) values with decreasing Ca values as a result of dilution (Fig. 6). When the glaciers were in a retreating or up-valley phase, they entrained sediment with higher Ca and lower Ti values.

5.2. *The early Holocene (∼12.0–8.0 ka)*

Glaciers throughout the southern tropical Andes retreated at the end of the Lateglacial stage (Seltzer et al., 2002), and the early Holocene was likewise a period of ice retreat in the southern tropical Andes (Fig. 10). In addition to warming (Weng et al., 2006), the stable isotope record from Lake Junin and palynological records from the region document a period of decreased effective moisture during the early Holocene (Seltzer et al., 1998, 2000; Bush et al., 2005; Hillyer et al., 2009). During this time, conditions were also more arid over the Altiplano (Rowe et al., 2002) and the Amazon Basin (Mosblech et al., 2012), indicating that a period of drier conditions was widespread across the region. Paleoglacier margins below Lake Jahuacocha were dated to the Lateglacial stage (Fig. 3), and the moraine that impounds Jahuacocha dates to ∼10.1 ± 0.9 ka based on the cosmogenic ^{10}Be of erratics on moraine crests (Hall et al., 2009). These ages combined with basal ages from the Jahuacocha sediment core (Table 1 & Fig. 8) suggest that the lake formed soon after the early Holocene glacier retreated upvalley, and that the glacier terminus subsequently remained above that elevation. There is tentative evidence based on moraine chronologies from southern Peru of an early Holocene glacier advance at some locations that interrupted the overall pattern of reduced ice cover (Licciardi et al., 2009), but more work is needed to verify that such an event occurred throughout the tropical Andes (Rodbell et al., 2009). The headwall of the Queshquecocha valley is at an intermediate elevation (5580 m asl) compared to the other lakes discussed here, and the clastic sediment values are consistently low through most of the early Holocene, indicating glaciers were restricted to relatively high elevations in the catchment. The moraines that have been dated upvalley of Laguna Queshquecocha are either of Lateglacial stage (Farber et al., 2005) or late Holocene age (Rodbell, 1992), and there is no evidence of a pronounced early Holocene ice advance. Further south in the Tuco and Jeullesh valleys of the Cordillera Blanca, exposure ages on moraines likewise indicate that glaciers were upvalley of their Lateglacial positions during the early Holocene (Glasser et al., 2009). Similarly, glaciers in the Cordillera Raura seem to have retreated during the early Holocene, as clastic sediment values in the Lutacocha sediment record progressively decrease, and no evidence of a pronounced ice advance has been documented in that valley.

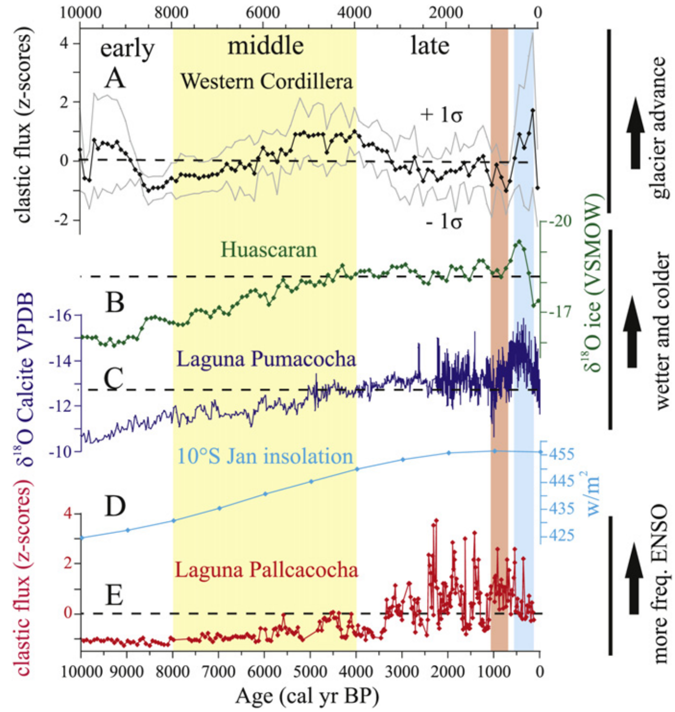

Fig. 10. (A) Stacked clastic flux *z*-scores for Lagunas Queshquecocha, Jahuacocha, Huarmicocha and Lutacocha (all with headwall elevations >5000 m asl) are compared to regional paleoclimate proxy records (B–E). Shading in yellow is for the middle Holocene, red is for the MCA and blue is for the LIA. Glacial variability generally tracks (B) colder and/or wetter conditions recorded in the Huascaran ice core (Thompson et al., 1995) and (C) stronger monsoon conditions recorded in the Laguna Pumacocha stable isotope record during the early and middle Holocene (Bird et al., 2011a). Ice margins then retreated under wetter conditions as implied by the stable isotope records and confirmed by lake level records (Abbott et al., 1997; Bird et al., 2011a) from ∼4 ka until the LIA. Glaciers advanced in many locations of the southern tropical Andes during the relatively cold and wet LIA. (D) The overall pattern of glacial variability is out-of-phase with summer insolation which is thought to cause wetter conditions during periods of high tropical insolation (Berger and Loutre, 1991). (E) ENSO events generally become more frequent during the late Holocene (Moy et al., 2002) when clastic sediment values in proglacial lakes decrease.

5.3. *The middle Holocene (∼8.0–4.0 ka)*

The paleoclimate records presented in this compilation document major climatic changes in the southern tropical Andes, featuring a shift to colder and wetter conditions during the middle Holocene in the western Cordillera. This interval also marks the "Neoglacial" phase of glacial resurgences starting at ∼5.0 ka in most mountainous regions around the globe, including the Southern Hemisphere (Porter and Denton, 1967; Porter, 2000). Wetter conditions in central Peru during the middle Holocene are apparent in the Laguna Pumacocha stable isotope record (Fig. 10), the Azulcocha lake level record (Bird et al., 2011a) and palynological records (Hillyer et al., 2009). Higher precipitation amounts alone, however, likely do not fully explain the magnitude of glacier advances that occurred at that time, and sharply changing clastic flux records provide supporting evidence of other observations that temperatures became abruptly colder at ∼5 ka (Thompson et al., 2006). For example, Lake Pacococha (4925 m), located on the northwest side of the Quelccaya Ice Cap in southern Peru, shows clastic sediment flux sharply increased around 5.2 ka, reaching its maximum for the Holocene at ∼4 ka (Rodbell et al., 2008). Radiocarbon-dated ice positions around Quelccaya also suggest that the ice cap was at a smaller extent than present from ∼7.0 to 5.2 ka (Mark et al., 2002; Buffen et al., 2009) before ice abruptly advanced at ∼5 ka (Buffen et al., 2009). In addition, the Lutacocha sediment record presented here contains an increasing trend of clastic sediment flux and glacial flour input that started at ~6.0 ka and peaked between ~5.0 and 4.0 ka. Likewise, the clastic sediment flux from Jahuacocha (Fig. 8) and Huarmicocha (Rodbell et al., 2008) have peak values during the middle Holocene at ~5.0 ka, followed by lower values thereafter. A prominent moraine is situated above Jahuacocha (Fig. 3), and although this feature has not been dated, it likely corresponds to the timing of peak clastic sediment flux into the lake during the middle and late Holocene. It should be noted, however, that this moraine is likely a compound feature produced by multiple Holocene advances, and future work should improve the chronology of this large moraine. Although less pronounced than in other records presented here, the clastic sediment profiles for Laguna Queshquecocha reach near-peak Holocene values between ~4.7 and 4.0 ka.

Records from the Bolivian Andes and the Amazon Basin provide additional evidence of shifting climatic conditions across the region during the middle Holocene. At nearly the same time that we observe increased clastic sediment flux in multiple records from the western Cordillera of the southern tropical Andes, the Sajama ice core dust profile suggests that conditions from ~6 to 4.0 ka were extremely arid on the Bolivian Altiplano (Thompson et al., 1998), and stable isotope records of speleothems from the Amazon Basin indicate generally drier conditions (Cruz et al., 2009; Strikis et al., 2011). Likewise, the water level record from Lake Titicaca indicates that the lowest lake levels of the Holocene occurred from ~6 to 4 ka (Rowe et al., 2002, 2003). Further evidence for dry conditions to the south can be found in the sediment record from Lake Taypi Chaki Khota located at 4300 m in the Cordillera Real of Bolivia, which shows a pronounced arid interval from ~8.5 to 2.5 ka and strong evidence that glaciers were absent from the watershed until after ~2.3 ka (Abbott et al., 2000). Combined, the lake level and glacial records from Bolivia suggest that the middle Holocene was drier to the south in the Andes compared with the western Cordillera of Peru.

5.4. The late Holocene (after ~4.0 ka)

Clastic sediment records from the western Cordillera indicate that glaciers retreated under warmer and wetter conditions at the start of the late Holocene at ~4.0 ka. For example, a transition is apparent in the Jahuacocha record, as multiple geochemical proxies for glacial flour show a decreasing trend after ~4.0 ka. Likewise, a basal age from a bog near Jahuacocha dates to 3.5 ka (Hall et al., 2009) and marks a period of ice retreat in the region (Fig. 3). Clastic sediment flux to Pacococha decreased after ~4 ka (Rodbell et al., 2008), and a similar phase of ice retreat in a valley near Quelccaya likely began at about this time (Mercer and Palacios, 1977; Mark et al., 2002). A similar major transition at ~3.8 ka in the Lutacocha valley is marked in the sediment core as a shift from massive, dark gray and dense sediment before 3.8 ka to finely laminated, lighter colored and less dense sediments through most of the remaining Holocene. The laminated nature of this sediment suggests that conditions during this interval were wetter and lake levels were higher during the late Holocene. Clastic sediment concentrations fluctuate and generally decrease in this laminated section of the Lutacocha core, providing further evidence that ice retreated under warmer and wetter conditions at times during the late Holocene. Interestingly, multiple proxies for clastic sediments in the Queshquecocha record remained relatively high during the late Holocene, suggesting that glacier and sediment processes fluctuated differently in that valley compared to the other records presented here.

It should be noted that whereas clastic sediment flux values were generally lower after 4.0 ka in the majority of the sediment records presented here, there were several notable increases in clastic sediments in individual records that occurred on multidecadal to centennial time-scales during the late Holocene. These sections of higher clastic flux may reflect intervals of expanded ice cover that have been independently documented for this period. For example, Clapperton (1972, 1983) reported a radiocarbon age for peat capped by till in the Cordillera Raura that dates to 2.5 ± 0.8 ka (Fig. 4). Similarly, Clapperton (1983) reported unpublished ages of Röthlisberger that date a glacial advance in the Cordillera Blanca to sometime between ~3.8 and 1.1 ka (3470 ± 215 and 1195 ± 60 ^{14}C BP). Moreover, Röthlisberger (1987) reported a maximum age of ~1.5 ka (1500 ± 200 ^{14}C BP) for a late Holocene ice advance from a buried soil in a moraine in the Cordillera Blanca that is similar to a maximum limiting age for an ice advance of 1.5 ka (1575 ± 170 ^{14}C BP) from a moraine composed of folded peat in the Cordillera Blanca (Rodbell, 1992). These latter ages correspond to the timing of pronounced, but relatively short-lived, increases in clastic sediment flux to the proglacial lakes in the western Cordillera. It is also noteworthy that a sediment record collected from the lake that sits above Laguna Queshquecocha suggests a major pulse of clastic sedimentation occurred at ~1.5 ka (Rodbell et al., 2008). However, it is not clear, based on these new records, if the radiocarbon dating of this sediment pulse is accurate, and it is possible that it corresponds to the LIA. Nevertheless, multiple moraine records suggest that ice advances occurred in the southern tropical Andes during and after the middle Holocene.

5.5. Medieval Climate Anomaly and Little Ice Age climate in the southern tropical Andes

The Medieval Climate Anomaly (1.0–0.7 ka) and Little Ice Age (0.6–0.1 ka) refer to climatic events that are well documented in the Northern Hemisphere (Mann et al., 2009). While there are leads and lags between glacial fluctuations in different parts of the world, it is clear that climatic changes affected other regions, including the southern tropics, during this interval (Thompson et al., 2006). Proxy climate records from the southern tropical Andes are generally consistent and suggest that conditions were relatively arid and likely warmer during the MCA compared to the rest of the Holocene. For example, clastic sediment flux was low in all of the lake sediment records presented in this study, as glaciers apparently retreated from ~1.0 to 0.7 ka. During this phase of mountain glacier retreat, δ^{18}O values in multiple records indicate a weaker SASM at the start of the MCA (Vuille et al., 2012). Moreover, multiple ice core records in the tropical Andes suggest that conditions were dry and warm relative to the LIA (Thompson et al., 2006).

Ice core records, lake sediment studies and glacial-geologic evidence indicate that a pronounced climatic shift occurred in the southern tropical Andes correlative with the LIA (Fig. 10). The clastic sediment records presented here suggest that glaciers advanced starting at ~0.6 ka, and retreated in the latter stages of the LIA. The ice core record from the Quelccaya ice cap indicates that there was a cold and wet phase from 0.5 to 0.2 ka, followed by a cold and dry phase that lasted for ~150 years (Thompson et al., 1986; Liu et al., 2005). Late Holocene moraine ages in the nearby Vilcabamba Range suggest that ice accumulated during the preceding wetter period recorded at Quelccaya, and then retreated later as conditions became more arid (Licciardi et al., 2009). Similarly, lichenometric studies of late Holocene moraines in the Cordillera Blanca yield ages from ~0.5 to 0.2 ka (Solomina et al., 2007; Jomelli et al., 2009). The lacustrine oxygen isotope record from Pumacocha in the central Andes indicates a wet phase occurred during the LIA that is similar to the isotope records from ice cores from Nevado Huascarán in the Cordillera Blanca and from the Quelccaya ice cap (Bird et al., 2011b). Evidence of a period of increased moisture at that time is also supported by higher water levels in Lake Titicaca from ~0.6 ka to the present (Abbott et al., 1997; Binford et al., 1997). Collectively, this evidence suggests that glaciers advanced under cold and wet conditions early in the LIA and retreated when conditions became warmer and drier in the latter stages of the LIA.

5.6. Stable isotopic versus mountain glacier records in the southern tropical Andes

Although there is considerable variability among the different clastic sediment records presented here, it is apparent that the stacked composite record (Fig. 10) represents a regional perspective that minimizes basin-scale influences, and improves the signal-to-noise ratio of the collective datasets. Glacier mass-balance changes in the western Cordillera of central Peru are driven by shifts in both water availability and temperature (Hastenrath, 1967; Kaser et al., 1990; Ames and Hastenrath, 1996; Dornbusch, 1998; Mark and Seltzer, 2005), and this study provides an opportunity to compare this composite of Holocene mountain glacier records with independently dated, high-resolution paleoclimate proxies. For example, stable isotope records from lacustrine sediments, speleothems and ice cores span the Holocene and provide evidence of shifting climatic conditions that can be compared to the clastic sediment records from the western Cordillera, and lake level studies to provide greater context. Although the climatic interpretation of oxygen isotope data in Andean ice records is debatable (Vuille et al., 2012), $\delta^{18}O$ values from ice cores provide evidence of shifting temperature and/or precipitation patterns since the Lateglacial stage (Thompson et al., 1985, 1995). On the other hand, precipitation amounts and the degree of rainout over the Amazon Basin remain the primary control on $\delta^{18}O$ in speleothems (Kanner et al., 2012), and open-basin lakes, such as Pumacocha, in the tropical Andes. With these considerations in mind, it has been argued that the $\delta^{18}O$ signal in both lacustrine sediments and speleothems represents changes in precipitation dynamics rather than shifts in atmospheric temperature (Bird et al., 2011a; Vuille et al., 2012). Interestingly, however, whereas the trend toward progressively more negative $\delta^{18}O$ values in open-basin lakes, speleothems and ice cores through the early Holocene is similar to the general pattern of advancing ice margins presented here (Fig. 10), there are marked differences in stable isotope and mountain glacier records during the middle to late Holocene. Most notably, the clastic sediment records suggest that glaciers retreated in the western Cordillera during the late Holocene, at a time stable isotope archives suggest greater precipitation amounts in this region of the Andes (Bird et al., 2011a). Further, lake level records (e.g. Abbott et al., 1997; Bird et al., 2011a) confirm the timing of positive changes in water availability. Lake Pumacocha is on the eastern slope of the Andes, and enhanced rainout across moisture gradients might explain part of the divergence at times between stable isotope and clastic sediment records (Polissar et al., 2006a), however, warmer atmospheric temperatures likely also contributed to the more negative glacier mass balance and a reduction in clastic sediment delivery to proglacial lake basins in the western Cordillera during the late Holocene. Thus, the mountain glacial records presented here provide a different perspective of climatic changes compared to the stable isotope archives currently available from the tropical Andes, and emphasize the additional role of temperature in driving glacier mass balance changes at times during the Holocene.

5.7. Glacier mass-balance and climate dynamics during the Holocene

Recent work shows that the tropical Pacific and North Atlantic Oceans influence inter-annual climate and circulation variability in tropical South America (Brienen et al., 2012), although the teleconnections and dynamical linkages between these systems are not well understood over Holocene time-scales. For example, summer (wet season) insolation values in the southern tropics were at a minimum during the early Holocene (Fig. 10) and likely led to weakened moisture convergence and reduced cloud cover over the Andes. Summer insolation values increased progressively during the Holocene, leading to a generally stronger SASM (i.e. higher precipitation and cloud cover), resulting in less radiation at the ice surface and a more positive glacier mass-balance (Favier et al., 2004). Ultimately, these complex non-linear climatic responses and feedbacks to insolation changes likely contributed Holocene temperature and precipitation variability throughout the tropical Andes (Seltzer et al., 2000).

Variability in tropical Pacific sea-surface temperatures (SSTs) likely influenced glacier mass balance changes in the southern tropical Andes during the Holocene by causing both temperature and precipitation changes at altitude. Atmospheric freezing heights respond to changes in the tropical Pacific as warmer SSTs lead to a more negative glacier mass-balance for low-elevation glaciers (Bradley et al., 2009). Today, changes in precipitation amounts are also associated with changes in the phase of ENSO through its impact on zonal flow anomalies that affect the tropical Andes as well as the position of the ITCZ over the tropical Atlantic (Münnich and Neelin, 2005; Vuille et al., 2008b; Garreaud et al., 2009). It is noteworthy that glaciers retreated in the western Cordillera during the late Holocene when ENSO events were enhanced relative to the early to middle Holocene (Rodbell et al., 1999; Moy et al., 2002; Loubere et al., 2013). Further, mean state changes in Pacific SSTs occurred that appear as prolonged periods of enhanced El Niño or La Niña during the late Holocene (Mann et al., 2009), although a robust dynamical link between ENSO and tropical glacial variability over longer time-scales remains unclear. We also note that North Atlantic SSTs are capable of driving climatic conditions in the southern tropical Andes through their role in ITCZ and monsoon dynamics (Baker et al., 2001). However, there are few high-resolution SST records from the Atlantic and Pacific Oceans available for testing these hypotheses, and more detailed paleoclimate records from both basins are needed in order to better evaluate how these systems are linked to tropical glacier mass-balance changes. Moreover, whereas considerable advancements have been made, fundamental questions remain regarding the timing and pattern of climatic changes in the tropical Andes that need to be addressed through the development of high-resolution proxy records and modeling studies in alpine regions. In particular, records of precipitation variability that span moisture gradients across the Andes are needed to quantitatively evaluate the dynamics and teleconnections that drive glacial and climatic variability in the Andes.

6. Conclusions

Clastic sediment records from the western Cordillera of the Peruvian Andes, combined with other proxy evidence from radiometrically dated ice positions, lake level changes, stable isotope archives, and palynological evidence indicate multiple phases of glaciation occurred during the Holocene in response to changing climatic conditions. The early Holocene was a period of generally reduced ice extent under relatively arid and warm conditions. The climate of the central Peruvian Andes during the middle Holocene underwent large-scale changes as evidenced by clastic sediment and glacial flour values peaking during colder and wetter conditions of the middle Holocene between ~8 and 4 ka, followed by a decreasing trend in several catchments until the latest Holocene. The lower alpine glaciers in the Cordillera Real of Bolivia were gone through the early and middle Holocene, not returning until after 2.2 ka, suggesting that glaciers further to the south were responding differently at this time. Notably, stable isotope records and lake level studies suggest that the amount of precipitation that reached the southern tropical Andes increased during the middle to late Holocene concurrent with reduced clastic sediment flux values in the Western Cordillera, suggesting that warmer conditions might have contributed to this phase of ice retreat. Although temperature likely continued to play a compounding role during the last millennium, multiple proxy records from the across the southern tropical Andes suggest that glaciers retreated during the relatively dry MCA, and advanced during the wet LIA.

Shifting tropical Pacific and North Atlantic ocean-atmospheric conditions likely contributed to temperature and precipitation changes in the Andes at times during the Holocene that in turn, influenced the pattern of glacial variability observed in the western Cordillera. Although the acquisition of recent proxy records has improved our understanding of the timing of glacial variability in the tropical Andes during the Holocene, more work is needed in order to understand the relative contributions of temperature and precipitation changes on glacier fluctuations. Moreover, the dynamical, synoptic-scale, controls on these climatic fluctuations need to be further explored through additional proxy records and modeling studies, especially regarding how these changes varied spatially across moisture gradients in the Andes.

Acknowledgments

We thank Daniel Bain, Broxton Bird, Patrick Burns, Colin Cooke, Alejandro Chu, Joanne Dalakos, Chris Moy, David Pompeani, Chris Sedlak, Michael Shoenfelt and Jacquie Smith for their assistance in the field and laboratory. Mark Brenner and an anonymous reviewer provided helpful comments that improved this manuscript. This paper also benefited from constructive comments by Lonnie Thompson and Paolo Gabrielli. This project was supported by the National Science Foundation Earth System History (AGS-0502464 & AGS-0502227) and Paleo-Perspectives on Climate Change (EAR-1003780 & EAR-1003711) programs. Additional funding was provided by the Ohio State University, Climate Water and Carbon Program. This is Contribution #1432 of the Byrd Polar Research Center.

References

Abbott, M.B., Binford, M.W., Brenner, M., Kelts, K.R., 1997. A 3500 C-14 yr high-resolution record of water-level changes in lake Titicaca, Bolivia/Peru. Quaternary Research 47, 169–180.

Abbott, M.B., Stafford, T.W., 1996. Radiocarbon geochemistry of modern and ancient Arctic lake systems, Baffin Island, Canada. Quaternary Research 45, 300–311.

Abbott, M.B., Wolfe, B.B., Aravena, R., Wolfe, A.P., Seltzer, G.O., 2000. Holocene hydrological reconstructions from stable isotopes and paleolimnology, Cordillera Real, Bolivia. Quaternary Science Reviews 19, 1801–1820.

Abbott, M.B., Wolfe, B.B., Wolfe, A.P., Seltzer, G.O., Aravena, R., Mark, B.G., Polissar, P.J., Rodbell, D.T., Rowe, H.D., Vuille, M., 2003. Holocene paleohydrology and glacial history of the central Andes using multiproxy lake sediment studies. Palaeogeography, Palaeoclimatology, Palaeoecology 194, 123–128.

Ames, A., Hastenrath, S.L., 1996. Diagnosing the imbalance of glacier Santa Rosa, Cordillera Raura, Peru. Journal of Glaciology 42, 212–218.

Baker, P.A., Seltzer, G., Fritz, S., Dunbar, R.B., Grove, M.J., Tapia, P.M., Cross, S.L., Rowe, H.D., Broda, J.P., 2001. The history of South American tropical precipitation for the past 25,000 years. Science 291, 640–643.

Benn, D.I., Owen, L.A., Finkel, R.C., Clemmens, S., 2006. Pleistocene lake outburst floods and fan formation along the eastern Sierra Nevada, California: implications for the interpretation of intermontane lacustrine records. Quaternary Science Reviews 25, 2729–2748.

Berger, A., Loutre, M.F., 1991. Insolation values for the climate of the last 10 million years. Quaternary Science Reviews 10, 297–317.

Binford, M.W., Kolata, A.L., Brenner, M., Janusek, J.W., Seddon, M.T., Abbott, M., Curtis, J.H., 1997. Climate variation and the rise and fall of an Andean civilization. Quaternary Research 47, 235–248.

Bird, B.W., Abbott, M.B., Rodbell, D.T., Vuille, M., 2011a. Holocene tropical South American hydroclimate revealed from a decadally resolved lake sediment d18O record. Earth and Planetary Science Letters 310, 192–202.

Bird, B.W., Abbott, M.B., Vuille, M., Rodbell, D.T., Stansell, N.D., Rosenmeier, M.F., 2011b. A 2,300-year-long annually resolved record of the South American summer monsoon from the Peruvian Andes. Proceedings of the National Academy of Sciences 108 (21), 8583–8588.

Bradley, R.S., Keimig, F., Diaz, H.F., Hardy, D.R., 2009. Recent changes in freezing level heights in the Tropics with implications for the deglacierization of high mountain regions. Geophysical Research Letters 36.

Bradley, R.S., Vuille, M., Hardy, D., Thompson, L.G., 2003. Low latitude ice cores record Pacific sea surface temperatures. Geophysical Research Letters 30, 1174.

Brienen, R.J.W., Helle, G., Pons, T.L., Guyot, J.-L., Gloor, M., 2012. Oxygen isotopes in tree rings are a good proxy for Amazon precipitation and El Niño-Southern Oscillation variability. Proceedings of the National Academy of Sciences 109 (42), 16957–16962.

Bronk Ramsey, C., 2008. Deposition models for chronological records. Quaternary Science Reviews 27, 42–60.

Buffen, A.M., Thompson, L.G., Mosley-Thompson, E., Huh, K.I., 2009. Recently exposed vegetation reveals Holocene changes in the extent of the Quelccaya Ice Cap, Peru. Quaternary Research 72, 157.

Bush, M.B., Hansen, B.C.S., Rodbell, D.T., Seltzer, G.O., Young, K.R., León, B., Abbott, M.B., Silman, M.R., Gosling, W.D., 2005. A 17 000-year history of Andean climate and vegetation change from Laguna de Chochos, Peru. Journal of Quaternary Science 20, 703–714.

Chiessi, C.M., Mulitza, S., Pätzold, J., Wefer, G., Marengo, J.A., 2009. Possible impact of the Atlantic Multidecadal Oscillation on the South American summer monsoon. Geophysical Research Letters 36, L21707.

Clapperton, C.M., 1972. The Pleistocene moraine stages of west-central Peru. Journal of Glaciology 11, 255–263.

Clapperton, C.M., 1983. The glaciation of the Andes. Quaternary Science Reviews 2, 83–155.

Clapperton, C.M., 1993. Quaternary Geology and Geomorphology of South America. Elsevier, Amsterdam.

Cobbing, E.J., Garayar, S.J., 1998. Mapa geologico del cuadrangulo de Oyon. Ministerio de Energia y Minas, Instituto Geologico Minero y Metalurgico, Republica del Peru.

Cobbing, E.J., Pitcher, W.S., Wilson, J.J., Baldock, J.W., Taylor, W.P., McCourt, W., Snelling, N.J., 1981. The Geology of the Western Cordillera of Northern Peru, vol. 5. Overseas memoir of the Institute of Geological Sciences, London.

Coelho, C.A.S., Uvo, C.B., Ambrizzi, T., 2002. Exploring the impacts of the tropical Pacific SST on the precipitation patterns over South America during ENSO periods. Theoretical and Applied Climatology 71, 185–197.

Coney, P.J., 1971. Structural evolution of the Cordillera Huayhuash, Andes of Peru. Geological Society of America Bulletin 82, 1863–1884.

Conley, D.J., 1998. An interlaboratory comparison for the measurement of biogenic silica in sediments. Marine Chemistry 63, 39–48.

Conley, D.J., Schelske, C.L., 2001. Biogenic silica. In: Smol, J.P., Birks, H.J., Last, W.M. (Eds.), Tracking Environmental Changes Using Lake Sediments. Terrestrial, Algal, and Siliceous Indicators. Springer.

Croudace, I.W., Rindby, A., Rothwell, R.G., 2006. ITRAX: Description and Evaluation of a New Multi-function X-ray Core Scanner. In: Geological Society, London, Special Publications, vol. 267, pp. 51–63.

Cruz, F.W., Vuille, M., Burns, S.J., Wang, X., Cheng, H., Werner, M., Lawrence Edwards, R., Karmann, I., Auler, A.S., Nguyen, H., 2009. Orbitally driven east-west antiphasing of South American precipitation. Nature Geosci 2, 210.

Dean, W.E., 1999. The carbon cycle and biogeochemical dynamics in lake sediments. Journal of Paleolimnology 21, 375–393.

DeMaster, D.J., 1979. The Marine Budgets of Silica and 32-Si. Yale University, New Haven.

DeMaster, D.J., 1981. The supply and accumulation of silica in the marine environment. Geochimica et Cosmochimica Acta 45, 1715–1732.

Dornbusch, U., 1998. Current large-scale climatic conditions in southern Peru and their influence on snowline altitudes. Erdkunde 52, 41–54.

Englemann, E.E., Jackson, L.L., Norton, D.R., Fischer, A.G., 1985. Determination of carbonate carbon in geological materials by coulometric titration. Chemical Geology 53, 125–128.

Fairman, M., 2006. Unpublished Master's thesis. The Ohio State University.

Farber, D.L., Hancock, G.S., Finkel, R.C., Rodbell, D.T., 2005. The age and extent of tropical alpine glaciation in the Cordillera Blanca, Peru. Journal of Quaternary Science 20, 759–776.

Favier, V., Wagnon, P., Ribstein, 2004. Glaciers of the outer and inner tropics: a different behaviour but a common response to climatic forcing. Geophysical Research Letters 31.

Francou, B., Ribstein, P., Saravia, R., Tiriau, E., 1995. Monthly balance and water discharge of an inter-tropical glacier: Zongo Glacier, Cordillera Real, Bolivia, 16°S. Journal of Glaciology 41, 61–67.

Garreaud, R.D., Vuille, M., Compagnucci, R., Marengo, J., 2009. Present-day south American climate. Palaeogeography, Palaeoclimatology, Palaeoecology 281, 180–195.

Glasser, N.F., Clemmens, S., Schnabel, C., Fenton, C.R., McHargue, L., 2009. Tropical glacier fluctuations in the Cordillera Blanca, Peru between 12.5 and 7.6 ka from cosmogenic 10Be dating. Quaternary Science Reviews 28, 3448.

Hall, S.R., Farber, D.L., Ramage, J.M., Rodbell, D.T., Finkel, R.C., Smith, J.A., Mark, B.G., Kassel, C., 2009. Geochronology of Quaternary glaciations from the tropical Cordillera Huayhuash, Peru. Quaternary Science Reviews 28, 2991.

Harbor, J.O.N., Warburton, J., 1992. Glaciation and denudation rates. Nature 356, 751.
Hastenrath, S., 2009. Past glaciation in the tropics. Quaternary Science Reviews 28, 790.
Hastenrath, S.L., 1967. Observations on the snow line in the Peruvian Andes. Journal of Glaciology 6, 541–550.
Henderson, K.A., Thompson, L.G., Lin, P.N., 1999. Recording El Nino in ice core d18O records from Nevado Huascaran, Peru. Journal of Geophysical Research 104, 31,053–031,065.
Hillyer, R., Valencia, B.G., Bush, M.B., Silman, M.R., Steinitz-Kannan, M., 2009. A 24,700-yr paleolimnological history from the Peruvian Andes. Quaternary Research 71, 71–82.
IPCC, 2007. Climate change 2007: impacts, adaptation and vulnerability. In: Parry, M.L., Canziani, O.F., Palutikof, J.P., van der Linden, P.J., Hanson, C.E. (Eds.), Contribution of Working Group II to the Fourth Assessment Report of the Intergovernmental Panel on Climate Change. Cambridge University Press, Cambridge, UK, p. 976.
Jansson, P., Rosqvist, G., Schneider, T., 2005. Glacier fluctuations, suspended sediment flux and glacio-lacustrine sediments. Geografiska Annalar 87 A, 37–50.
Johnson, A.M., 1976. The climate of Peru, Bolivia and Ecuador. In: Schwerdtfeger, W. (Ed.), World Survey of Climatology. Climates of Central and South America, vol. 12. Elsevier.
Jomelli, V., Favier, V., Rabatel, A., Brunstein, D., Hoffmann, G., Francou, B., 2009. Fluctuations of glaciers in the tropical Andes over the last millennium and palaeoclimatic implications: a review. Palaeogeography, Palaeoclimatology, Palaeoecology 281, 269–282.
Kanner, L.C., Burns, S.J., Cheng, H., Edwards, R.L., 2012. High-latitude forcing of the south American summer monsoon during the last glacial. Science 335, 570–573.
Kaser, G., Ames, A., Zamora, M., 1990. Glacier fluctuations and climate in the cordillera Blanca, Peru. Annals of Glaciology 14, 136–140.
Kaser, G., Georges, C., 1997. Changes of the equilibrium-line altitude in the tropical Cordillera Blanca, Peru, 1930–1950, and their spatial variations. Annals of Glaciology 24, 344–349.
Kaser, G., Juen, I., Georges, C., Gomez, J., Tamayo, W., 2003. The impact of glaciers on the runoff and the reconstruction of mass balance history from hydrological data in the tropical Cordillera Blanca, Peru. Journal of Hydrology 282, 130–144.
Kaser, G., Osmaston, H., 2002. Tropical Glaciers. Cambridge University Press, Cambridge.
Lawrimore, J.H., Menne, M.J., Gleason, B.E., Williams, C.N., Wuertz, D.B., Vose, R.S., Rennie, J., 2011. An overview of the Global Historical Climatology Network monthly mean temperature data set, version 3. Journal of Geophysical Research 116, D19121.
Leonard, E.M., 1997. The relationship between glacial activity and sediment production: evidence from a 4450-year varve record of Neoglacial sedimentation in Hector Lake, Alberta, Canada. Journal of Paleolimnology 17, 319–330.
Licciardi, J.M., Schaefer, J.M., Taggart, J.R., Lund, D.C., 2009. Holocene glacier fluctuations in the Peruvian Andes indicate northern climate linkages. Science 325, 1677–1679.
Liu, K., Resse, C.A., Thompson, L.G., 2005. Ice-core pollen record of climatic changes in the central Andes during the last 400 yr. Quaternary Research 64, 272–278.
Loubere, P., Creamer, W., Haas, J., 2013. Evolution of the El Nino-Southern Oscillation in the late Holocene and insolation driven change in the tropical annual SST cycle. Global and Planetary Change 100, 129–144.
Mann, M.E., Zhang, Z., Rutherford, S., Bradley, R.S., Hughes, M.K., Shindell, D., Ammann, C., Faluvegi, G., Ni, F., 2009. Global Signatures and dynamical origins of the little ice age and Medieval climate Anomaly. Science 326, 1256–1260.
Mark, B.G., Seltzer, G.O., 2005. Evaluation of recent glacier recession in the Cordillera Blanca, Peru (AD 1962–1999): spatial distribution of mass loss and climatic forcing. Quaternary Science Reviews 24, 2265.
Mark, B.G., Seltzer, G.O., Rodbell, D.T., Goodman, A.Y., 2002. Rates of deglaciation during the last glaciation and Holocene in the cordillera Vilcanota–Quelccaya ice cap region, Southeastern Peru. Quaternary Research 57, 287–298.
Maslin, M.A., Burns, S.J., 2000. Reconstruction of the Amazon basin effective moisture availability over the past 14,000 years. Science 290, 2285–2287.
Maslin, M.A., Ettwein, V.J., Wilson, K.E., Guilderson, T.P., Burns, S.J., Leng, M.J., 2011. Dynamic boundary-monsoon intensity hypothesis: evidence from the deglacial Amazon River discharge record. Quaternary Science Reviews 30, 3823–3833.
McFadden, E.M., Ramage, J., Rodbell, D.T., 2011. Landsat TM and ETM+ derived snowline altitudes in the Cordillera Huayhuash and Cordillera Raura, Peru, 1986–2005. The Cryosphere 5, 419–430.
McNulty, B., Farber, D., 2002. Active detachment faulting above the Peruvian flat slab. Geology 30, 567–570.
Mercer, J.H., Palacios, M.O., 1977. Radiocarbon dating of the last glaciation in Peru. Geology 5, 600–604.
Mosblech, N.A.S., Bush, M.B., Gosling, W.D., Hodell, D., Thomas, L., van Calsteren, P., Correa-Metrio, A., Valencia, B.G., Curtis, J., van Woesik, R., 2012. North Atlantic forcing of Amazonian precipitation during the last ice age. Nature Geoscience 5, 817–820.
Moy, C.M., 1998. Continuous Records of Late Holocene Paleoclimate Change as Interpreted from Sediment Provenance and a Lacustrine Sediment Core, Cordillera Blanca, Peru. Ph.D. thesis. Department of Geology, Union College, USA. p. 93.
Moy, C.M., Seltzer, G., Rodbell, D.T., Anderson, D., 2002. Variability of El Niño/Southern Oscillation activity at millennial timescales during the Holocene epoch. Nature 420, 162–165.
Münnich, M., Neelin, J.D., 2005. Seasonal influence of ENSO on the Atlantic ITCZ and equatorial South America. Geophysical Research Letters 32, L21709.
Nobre, P., Srukla, J., 1996. Variations of sea surface temperature, wind stress, and rainfall over the tropical Atlantic and south America. Journal of Climate 9, 2464–2479.
Nussbaumer, S.U., Steinhilber, F., Trachsel, M., Breitenmoser, P., Beer, Jürg, Blass, A., Grosjean, M., Hafner, A., Holzhauser, H., Wanner, H., Zumbühl, H.J., 2011. Alpine climate during the Holocene: a comparison between records of glaciers, lake sediments and solar activity. Journal of Quaternary Science 26, 703–713.
Oldfield, F., Appleby, P.G., 1984. Empirical testing of 210Pb-dating models for lake sediments. In: Haworth, E.Y., Lund, J.W.G. (Eds.), Lake Sediments and Environmental History. University of Minnesota, Minneapolis, MN.
Polissar, P.J., Abbott, M.B., Shemesh, A., Wolfe, A.P., Bradley, R.S., 2006a. Holocene hydrologic balance of tropical South America from oxygen isotopes of lake sediment opal, Venezuelan Andes. Earth and Planetary Science Letters 242, 375.
Polissar, P.J., Abbott, M.B., Wolfe, A.P., Bezada, M., Rull, V., Bradley, R.S., 2006b. Solar modulation of Little Ice Age climate in the tropical Andes. Proceedings of the National Academy of Sciences 103, 8937–8942.
Porter, S.C., 2000. Onset of Neoglaciation in the southern Hemisphere. Journal of Quaternary Science 15, 395–408.
Porter, S.C., Denton, G.H., 1967. Chronology of Neoglaciation in the North American Cordillera. American Journal of Science 265, 177–210.
Rabatel, A., Francou, B., Soruco, A., Gomez, J., CÃ¡ceres, B., Ceballos, J.L., Basantes, R., Vuille, M., Sicart, J.E., Huggel, C., Scheel, M., Lejeune, Y., Arnaud, Y., Collet, M., Condom, T., Consoli, G., Favier, V., Jomelli, V., Galarraga, R., Ginot, P., Maisincho, L., Mendoza, J., Ménégoz, M., Ramirez, E., Ribstein, P., Suarez, W., Villacis, M., Wagnon, P., 2013. Current state of glaciers in the tropical Andes: a multi-century perspective on glacier evolution and climate change. The Cryosphere 7, 81–102.
Reimer, P.J., Baillie, M.G.L., Bard, E., Bayliss, A., Beck, J.W., Blackwell, P.G., Bronk Ramsey, C., Buck, C.E., Burr, G.S., Edwards, R.L., Friedrich, M., Grootes, P.M., Guilderson, T.P., Hajdas, I., Heaton, T.J., Hogg, A.G., Hughen, K.A., Kaiser, K.F., Kromer, B., McCormac, G., Reimer, R.W., Richards, D.A., Southon, J.R., Talamo, S., Turney, C.S.M., van der Plicht, J., Weyhenmeyer, C., 2009. IntCal09 and Marine09 radiocarbon age calibration curves, 0–50,000 years cal BP. Radiocarbon 51, 1111–1150.
Rodbell, D.T., 1991. Late Quaternary Glaciation and Climatic Change in the Northern Peruvian Andes. Unpublished PhD dissertation. University of Colorado.
Rodbell, D.T., 1992. Lichenometric and radiocarbon dating of Holocene glaciation, Cordillera Blanca, Perú. The Holocene 2, 19–29.
Rodbell, D.T., Seltzer, G.O., Anderson, D.M., Abbott, M.B., Enfield, D.B., Newman, J.H., 1999. An ~15,000-year record of El Niño-driven alluviation in southwestern Ecuador. Science 283, 516–520.
Rodbell, D.T., Seltzer, G.O., Mark, B.G., Smith, J.A., Abbott, M.B., 2008. Clastic sediment flux to tropical Andean lakes: records of glaciation and soil erosion. Quaternary Science Reviews 27, 1612–1626.
Rodbell, D.T., Smith, J.A., Mark, B.G., 2009. Glaciation in the Andes during the Late Glacial and Holocene. Quaternary Science Reviews 28, 2165–2212.
Röthlisberger, F., 1987. 10 000 Jahre Gletschergeschichte der Erde. Verlag Sauerlande, Aarau.
Rothwell, R.G., Rack, F.R., 2006. New Techniques in Sediment Core Analysis: an Introduction. In: New Techniques in Sediment Core Analysis Geological Society, London, Special Publications, vol. 267, pp. 1–29.
Rowe, H.D., Dunbar, R.B., Mucciarone, D.A., Seltzer, G.O., Baker, P.A., Fritz, S., 2002. Insolation, moisture balance and climate change on the South American Altiplano since the Last Glacial Maximum. Climatic Change 52, 175–199.
Rowe, H.D., Guilderson, T., Dunbar, R.B., Southon, J., Seltzer, G., Mucciarone, D.A., Fritz, S., Baker, P.A., 2003. Late Quaternary lake-level changes constrained by radiocarbon and stable isotope studies on sediment cores from Lake Titicaca, South America. Global and Planetary Change 38, 273–290.
Seltzer, G.O., 1992. Late Quaternary glaciation of the Cordillera Real, Bolivia. Journal of Quaternary Science 7, 87–98.
Seltzer, G.O., Baker, P., Cross, S., Dunbar, R., Fritz, S., 1998. High-resolution seismic reflection profiles from Lake Titicaca, Peru-Bolivia: evidence for Holocene aridity in the tropical Andes. Geology 26, 167–170.
Seltzer, G.O., Rodbell, D.T., Baker, P.A., Fritz, S.C., Tapia, P.M., Rowe, H.D., Dunbar, R.B., 2002. Early warming of tropical south America at the last glacial–interglacial transition. Science 296, 1685–1686.
Seltzer, G.O., Rodbell, D.T., Burns, S., 2000. Isotopic evidence for late Quaternary climatic change in tropical South America. Geology 28, 35–38.
Smith, N.D., Ashley, G.M., 1985. Proglacial lacustrine environment. In: Smith, N.D., Ashley, G.M. (Eds.), Glacial Sedimentary Environments.
Solomina, O., Jomelli, V., Kaser, G., Ames, A., Berger, B., Pouyaud, B., 2007. Lichenometry in the Cordillera Blanca, Peru: "Little Ice Age" moraine chronology. Global and Planetary Change 59, 225–235.
Stansell, N.D., 2009. Rapid Climate Change in the Tropical Americas during the Late-Glacial Interval and the Holocene. Unpublished PhD dissertation. University of Pittsburgh.
Stansell, N.D., Abbott, M.B., Polissar, P.J., Wolfe, A.P., Bezada, M., Rull, V., 2005. Late Quaternary deglacial history of the Mérida Andes, Venezuela. Journal of Quaternary Science 20, 801–812. http://dx.doi.org/10.1002/jqs.973.
Stansell, N.D., Abbott, M.B., Rull, V., Rodbell, D.T., Bezada, M., Montoya, E., 2010. Abrupt Younger Dryas cooling in the northern tropics recorded in lake sediments from the Venezuelan Andes. Earth and Planetary Science Letters 293, 154–163.

Stevens, K., 2004. A High-Resolution Glacial History of the Tropical Andes from Sediment Cores from Laguna Jahuacocha, Cordillera Huayhuash, Peru. Ph.D. thesis. Union College, USA.

Strikis, N.M., Cruz, F.W., Cheng, H., Karmann, I., Edwards, R.L., Vuille, M., Wang, X., de Paula, M.S., Novello, V.F., Auler, A.S., 2011. Abrupt variations in South American monsoon rainfall during the Holocene based on a speleothem record from central-eastern Brazil. Geology 39, 1075–1078.

Thompson, L.G., Davis, M.E., Mosley-Thompson, E., Sowers, T.A., Henderson, K.A., Zagorodnov, V.S., Lin, P.-N., Mikhalenko, V.N., Campen, R.K., Bolzan, J.F., Cole-Dai, J., Francou, B., 1998. A 25,000-year tropical climate history from Bolivian ice cores. Science 282, 1858–1864.

Thompson, L.G., Mosley-Thompson, E., Bolzan, J.F., Koci, B.R., 1985. A 1500-year record of tropical precipitation in ice cores from the Quelccaya ice cap, Peru. Science 229, 971–973.

Thompson, L.G., Mosley-Thompson, E., Brecher, H., Davis, M.E., Leon, B., Les, D., Lin, P.N., Mashiotta, t., Mountain, K., 2006. Abrupt tropical climate change: past and present. Proceedings of the National Academy of Sciences 103, 10536–10543.

Thompson, L.G., Mosley-Thompson, E., Dansgaard, W., Grootes, P.M., 1986. The Little Ice Age as recorded in the stratigraphy of the tropical Quelccaya ice cap. Science 234, 361–364.

Thompson, L.G., Mosley-Thompson, E., Davis, M.E., Lin, P.-N., Henderson, K.A., Cole-Dai, J., Bolzan, J.F., Liu, K.-b., 1995. Late glacial stage and Holocene tropical ice core records from Huascarán. Peru. Science 269, 46–50.

Trauth, M.H., 2010. Time-Series Analysis MATLAB® Recipes for Earth Sciences. Springer, Berlin Heidelberg, pp. 107–159.

Vuille, M., Bradley, R.S., Keimig, F., 2000. Interannual climate variability in the Central Andes and its relation to tropical Pacific and Atlantic forcing. Journal of Geophysical Research 105, 12,447–412,460.

Vuille, M., Burns, S.J., Taylor, B.L., C, F.W., Bird, B.W., Abbott, M.B., Kanner, L.C., Cheng, H., Novello, V.F., 2012. A review of the South America monsoon history as recorded in stable isotope proxies over the past two millennia. Climate of the Past 8, 1309–1321.

Vuille, M., Francou, B., Wagnon, P., Juen, I., Kaser, G., Mark, B.G., Bradley, R.S., 2008a. Climate change and tropical Andean glaciers: past, present and future. Earth-Science Reviews 89, 79–96.

Vuille, M., Kaser, G., Juen, I., 2008b. Glacier mass balance variability in the Cordillera Blanca, Peru and its relationship with climate and the large-scale circulation. Global and Planetary Change 62, 14–28.

Vuille, M., Werner, M., 2005. Stable isotopes in precipitation recording South American summer monsoon and ENSO variability observations and model results. Climate Dynamics 25, 401–413.

Weng, C., Bush, M.B., Curtis, J.H., Kolata, A.L., Dillehay, T.D., Binford, M.W., 2006. Deglaciation and Holocene climate change in the western Peruvian Andes. Quaternary Research 66, 87–96.

Wright, H.E., Mann, D.H., Glaser, P.H., 1984. Piston corers for peat and lake sediments. Ecology 65, 657–659.

Zhou, J., Lau, K.-M., 1998. Does a monsoon climate exist over south America? Journal of Climate 11, 1020–1040.